Operating System Management of MEMS-based Storage Devices

John Linwood Griffin, Steven W. Schlosser,
Gregory R. Ganger, David F. Nagle
Carnegie Mellon University

Abstract

MEMS-based storage devices promise significant performance, reliability, and power improvements relative to disk drives. This paper compares and contrasts these two storage technologies and explores how the physical characteristics of MEMS-based storage devices change four aspects of operating system (OS) management: request scheduling, data placement, failure management, and power conservation. Straightforward adaptations of existing disk request scheduling algorithms are found to be appropriate for MEMS-based storage devices. A new bipartite data placement scheme is shown to better match these devices' novel mechanical positioning characteristics. With aggressive internal redundancy, MEMS-based storage devices can mask and tolerate failure modes that halt operation or cause data loss for disks. In addition, MEMS-based storage devices simplify power management because the devices can be stopped and started rapidly.

1 Introduction

Decades of research and experience have provided operating system builders with a healthy understanding of how to manage disk drives and their role in storage systems. This management includes achieving acceptable performance despite relatively time-consuming mechanical positioning delays, dealing with transient and permanent hardware problems so as to achieve high degrees of data survivability and availability, and minimizing power dissipation in battery-powered mobile environments. To address these issues, a wide array of OS techniques are used, including request scheduling, data layout, prefetching, caching, block remapping, data replication, and device spin-down. Given the prevalence and complexity of disks, most of these techniques have been specifically tuned to their physical characteristics.

When other devices (e.g., magnetic tape or Flash RAM) are used in place of disks, the characteristics of the problems change. Putting new devices behind a disk-like interface is generally sufficient to achieve a working system. However, OS management techniques must be tuned to a particular device's characteristics to achieve the best performance, reliability, and lifetimes. For example, request scheduling techniques are much less important for RAM-based storage devices than for disks, since location-dependent mechanical delays are not involved. Likewise, locality-enhancing block layouts such as cylinder groups [18], extents [19], and log-structuring [24] are not as beneficial. However, log-structured file systems with idle-time cleaning can increase both performance and device lifetimes of Flash RAM storage devices with large erasure units [5].

Microelectromechanical systems (MEMS)-based storage is an exciting new technology that will soon be available in systems. MEMS are very small scale mechanical structures—on the order of 10–1000 μm—fabricated on the surface of silicon wafers [33]. These microstructures are created using photolithographic processes much like those used to manufacture other semiconductor devices (e.g., processors and memory) [7]. MEMS structures can be made to slide, bend, and deflect in response to electrostatic or electromagnetic forces from nearby actuators or from external forces in the environment. Using minute MEMS read/write heads, data bits can be stored in and retrieved from media coated on a small movable media sled [1, 11, 31]. Practical MEMS-based storage devices are the goal of major efforts at many research centers, including IBM Zurich Research Laboratory [31], Carnegie Mellon University [1], and Hewlett-Packard Laboratories [13].

Like disks, MEMS-based storage devices have unique mechanical and magnetic characteristics that merit specific OS techniques to manage performance, fault tolerance, and power consumption. For example, the mechanical positioning delays for MEMS-based storage devices depend on the initial and destination position and velocity of the media sled, just as disks' positioning times are dependent on the arm position and platter rotational offset. However, the mechanical expressions that characterize sled motion differ from those describing disk platter and arm motion. These differences impact both request scheduling and data layout trade-offs. Similar examples exist for failure management and power conservation mechanisms. To assist designers of both MEMS-based storage devices and the systems that use them, an understanding of the options and trade-offs for OS management of these devices must be developed.

This paper takes a first step towards developing this understanding of OS management techniques for MEMS-based storage devices. It focuses on devices with the movable sled design that is being developed independently by several groups. With higher storage densities (260–720 Gbit/in^2) and lower random access times (less than 1 ms) than disks, these devices could play a significant role in future systems. After describing a disk-like view of these devices, we compare and contrast their characteristics with those of disks. Building on these comparisons, we explore options and implications for three major OS management issues: performance (specifically, request scheduling and block layout), failure management (media defects, device failures, and host crashes), and power conservation.

While these explorations are unlikely to represent the final word for OS management of these emerging devices, we believe that several of our high-level results will remain valid:

- Disk scheduling algorithms can be easily adapted to MEMS-based storage devices, improving performance much like they do for disks.

- Disk layout techniques can be adapted usefully, but the Cartesian movement of the sled (instead of the rotational motion of disks) allows further refinement of layouts.

- Striping of data and error correcting codes (ECC) across tips can greatly increase a device's tolerance to media, tip, and electronics faults; in fact, many faults that would halt operation or cause data loss in disks can be masked and tolerated in MEMS-based storage devices.

- OS power conservation is much simpler for MEMS-based storage devices. In particular, miniaturization and lack of rotation enable rapid transition between power-save and active modes, obviating the need for complex idle-time prediction and maximization algorithms.

The remainder of this paper is organized as follows. Section 2 describes MEMS-based storage devices, focusing on how they are similar to and different from magnetic disks. Section 3 describes our experimental setup, including the simulator and the workloads used. Section 4 evaluates request scheduling algorithms for MEMS-based storage devices. Section 5 explores data layout options. Section 6 describes approaches to fault management within and among MEMS-based storage devices. Section 7 discusses other device characteristics impacting the OS. Section 8 summarizes this paper's contributions.

2 MEMS-based storage devices

This section describes a MEMS-based storage device and compares and contrasts its characteristics with those of conventional disk drives. The description, which follows that of Reference [11], maps these devices onto a disk-like metaphor appropriate to their physical and operational characteristics.

2.1 Basic device description

MEMS-based storage devices can use the same basic magnetic recording technologies as disks to read and write data on the media. However, because it is difficult to build reliable rotating components in silicon, MEMS-based storage devices are unlikely to use rotating platters. Instead, most current designs contain a movable sled coated with magnetic media. This *media sled* is spring-mounted above a two-dimensional array of fixed read/write heads (*probe tips*) and can be pulled in the X and Y dimensions by electrostatic actuators along each edge. To access data, the media sled is first pulled to a specific location (x,y displacement). When this seek is complete, the sled moves in the Y dimension while the probe tips access the media. Note that the probe tips remain stationary—except for minute X and Z dimension movements to adjust for surface variation and skewed tracks—while the sled moves. In contrast, rotating platters and actuated read/write heads share the task of positioning in disks. Figures 1 and 2 illustrate this MEMS-based storage device design.

As a concrete example, the footprint of one MEMS-based storage device design is 196 mm^2, with 64 mm^2 of usable media area and 6400 probe tips [1]. Dividing the media into bit cells of 40×40 nm, and accounting for an ECC and encoding overhead of 2 bits per byte, this design has a formatted capacity of 3.2 GB/device. Note the square nature of the bit cells, which is not the case in conventional disk drives. With minute probe tips and vertical record-

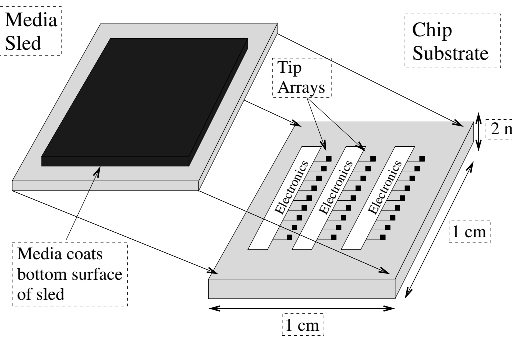

Figure 1: ***Components of a MEMS-based storage device.*** *The media sled is suspended above an array of probe tips. The sled moves small distances along the X and Y axes, allowing the stationary tips to address the media.*

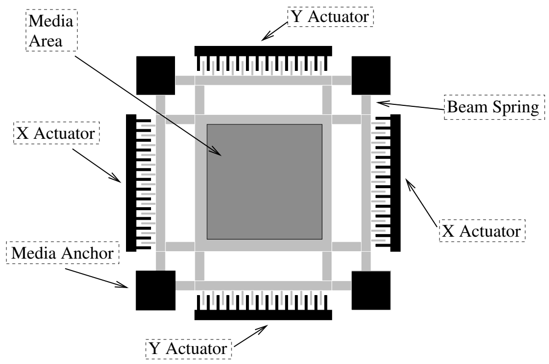

Figure 2: ***The movable media sled.*** *The actuators, spring suspension, and the media sled are shown. Anchored regions are solid and the movable structure is shaded grey.*

ing, bits stored on these devices can have a 1-to-1 aspect ratio, resulting in areal densities 15–30 times greater than those of disks. However, per-device capacities are lower because individual MEMS-based storage devices are much smaller than disks. Because the mechanically-positioned MEMS components have much smaller masses than corresponding disk parts, their random access times are in the hundreds of microseconds. For the default device parameters in this paper, the average random 4 KB access time is 703 μs.

2.2 Low-level data layout

The storage media on the sled is divided into rectangular regions as shown in Figure 3. Each region contains M×N bits (e.g., 2500×2500) and is accessible by exactly one probe tip; the number of regions on the media equals the number of probe tips. Each term in the nomenclature below is defined both in the text and visually in Figure 4.

Cylinders. Drawing on the analogy to disk terminology, we refer to a *cylinder* as the set of all bits with identical x offset within a region (i.e., at identical sled displacement in X). In other words, a cylinder consists of all bits accessible by all tips when the sled moves only in the Y dimension, remaining immobile in the X dimension. Cylinder 1 is highlighted in Figure 4 as the four circled columns of bits. This definition parallels that of disk cylinders, which consist of all bits accessible by all heads while the arm remains immobile. There are M cylinders per sled. In our default model, each sled has 2500 cylinders that each hold 1350 KB of data.

Tracks. A MEMS-based storage device might have 6400 tips underneath its media sled; however, due to power and heat considerations it is unlikely that all 6400 tips can be *active* (accessing data) concurrently. We expect to be able to activate 200–2000 tips at a time. To account for this limitation, we divide cylinders into tracks. A *track* consists of all bits within a cylinder that can be read by a group of concurrently active tips. The sled in Figure 4 has sixteen tips (one per region; not all tips are shown), of which up to four can be concurrently active—each cylinder therefore has four tracks. Track 0 of cylinder 1 is highlighted in the figure as the leftmost circled column of bits. Note again the parallel with disks, where a track consists of all bits within a cylinder accessible by a single active head. In our default model, each sled has 6400 tips and 1280 concurrently active tips, so each cylinder contains 5 tracks that each hold 270 KB of data. Excluding positioning time, accessing an entire track takes 3.47 ms.

Sectors. Continuing the disk analogy, tracks are divided into sectors. Instead of having each active tip read or write an entire vertical column of N bits, each tip accesses only 90 bits at a time—10 bits of servo/tracking information and 80 data bits (8 encoded data bytes). Each 80-data-bit group forms an 8-byte *sector*, which is the smallest individually accessible unit of data on our MEMS-based storage device. Each track in Figure 4 contains 12 sectors (3 per tip). These sectors parallel the partitioning of disk tracks into sectors, with three notable differences. First, disk sectors contain more data (e.g., 512 bytes vs. 8 bytes). Second, MEMS-based storage devices can access multiple sectors concurrently: Figure 4 shows the four active tips accessing sectors 4, 5, 6, and 7. Third, MEMS-based storage devices can support *bidirectional access*, meaning that a data sector can be accessed in either the +Y or

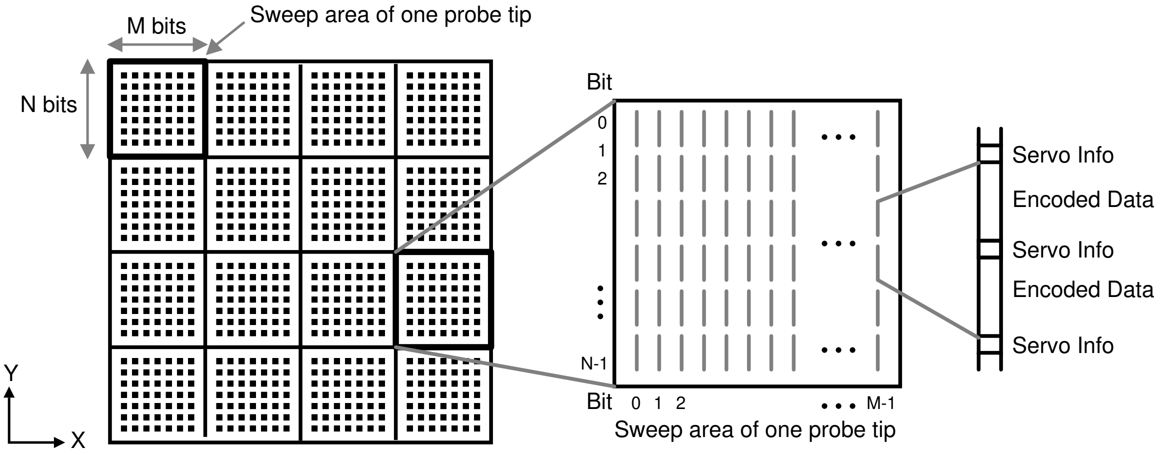

Figure 3: ***Data organization on MEMS-based storage devices.*** *The illustration depicts a small portion of the magnetic media sled. Each small rectangle outlines the media area accessible by a single probe tip, with a total of 16 tip regions shown. A full device contains thousands of tips and tip regions. Each region stores $M\times N$ bits, organized into M vertical columns of N bits, alternating between servo/tracking information (10 bits) and data (80 bits = 8 encoded data bytes). To read or write data, the media sled passes over the tips in the $\pm Y$ directions while the tips access the media.*

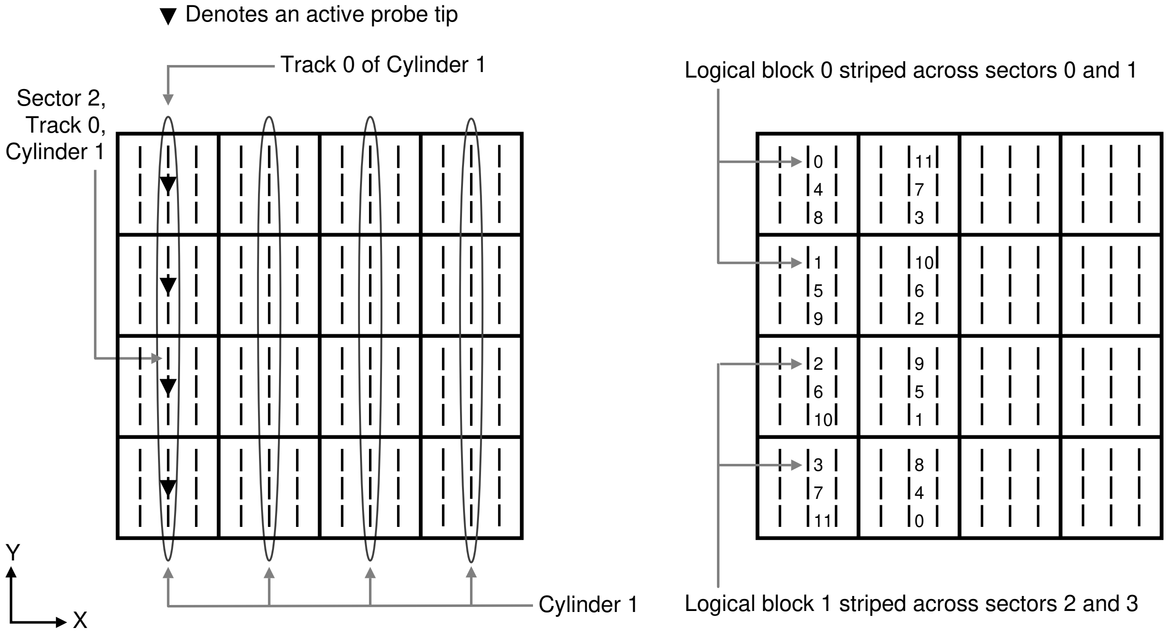

Figure 4: ***Cylinders, tracks, sectors, and logical blocks.*** *This example shows a MEMS-based storage device with 16 tips and $M\times N = 3\times 280$. A "cylinder" is defined as all data at the same* x *offset within all regions; cylinder 1 is indicated by the four circled columns of bits. Each cylinder is divided into 4 "tracks" of 1080 bits, where each track is composed of four tips accessing 280 bits each. Each track is divided into 12 "sectors" of 80 bits each, with 10 bits of servo/tracking information between adjacent sectors and at the top and bottom of each track. (There are nine sectors in each tip region in this example.) Finally, sectors are grouped together in pairs to form "logical blocks" of 16 bytes each. Sequential sector and logical block numbering are shown on the right. These definitions are discussed in detail in Section 2.2.*

$-$Y direction. In our default model, each track is composed of 34,560 sectors of 8 bytes each, of which up to 1280 sectors can be accessed concurrently. Excluding positioning time, each 1280 sector (10 KB) access takes 0.129 ms.

Logical blocks. For the experiments in this paper, we combine groups of 64 sectors into SCSI-like *logical blocks* of 512 bytes each. Each logical block is therefore striped across 64 tips, and up to 20 logical blocks can be accessed concurrently ($1280 \div 64 = 20$). During a request, only those logical blocks needed to satisfy the request and any firmware-directed prefetching are accessed; unused tips remain inactive to conserve power.

2.3 Media access characteristics

Media access requires constant sled velocity in the Y dimension and zero velocity in the X dimension. The Y dimension *access speed* is a design parameter and is determined by the per-tip read and write rates, the bit cell width, and the sled actuator force. Although read and write data rates could differ, tractable control logic is expected to dictate a single access velocity in early MEMS-based storage devices. In our default model, the access speed is 28 mm/s and the corresponding per-tip data rate is 0.7 Mbit/s.

Positioning the sled for read or write involves several mechanical and electrical actions. To seek to a sector, the appropriate probe tips must be activated (to access the servo information and then the data), the sled must be positioned at the correct x,y displacement, and the sled must be moving at the correct velocity for access. Whenever the sled seeks in the X dimension—i.e., the destination cylinder differs from the starting cylinder—extra *settling time* must be taken into account because the spring-sled system oscillates in X after each cylinder-to-cylinder seek. Because this oscillation is large enough to cause off-track interference, a closed loop settling phase is used to damp the oscillation. To the first order, this active damping is expected to require a constant amount of time. Although slightly longer settling times may ultimately be needed for writes, as is the case with disks, we currently assume that the settling time is the same for both read and write requests. Settling time is not a factor in Y dimension seeks because the oscillations in Y are subsumed by the large Y dimension access velocity and can be tolerated by the read/write channel.

As the sled is moved away from zero displacement, the springs apply a restoring force toward the sled's rest position. These spring forces can either improve or degrade positioning time (by affecting the effective actuator force), depending on the sled displacement and direction of motion. This force is parameterized in our simulator by the *spring factor*—the ratio of the maximum spring force to the maximum actuator force. A spring factor of 75% means that the springs pull toward the center with 75% of the maximum actuator force when the sled is at full displacement. The spring force decreases linearly to 0% as sled displacement approaches zero. The spring restoring force makes the acceleration of the sled a function of instantaneous sled position. In general, the spring forces tend to degrade the seek time of short seeks and improve the seek time of long seeks [11].

Large transfers may require that data from multiple tracks or cylinders be accessed. To switch tracks during large transfers, the sled switches which tips are active and performs a *turnaround*, using the actuators to reverse the sled's velocity (e.g., from +28 mm/s to $-$28 mm/s). The turnaround time is expected to dominate any additional activity, such as the time to activate the next set of active tips, during both track and cylinder switches. One or two turnarounds are necessary for any seek in which the sled is moving in the wrong direction—away from the sector to be accessed—before or after the seek.

2.4 Comparison to conventional disks

Although MEMS-based storage devices involve some radically different technologies from disks, they share enough fundamental similarity for a disk-like model to be a sensible starting point. Like disks, MEMS-based storage devices stream data at a high rate and suffer a substantial distance-dependent positioning time delay before each nonsequential access. In fact, although MEMS-based storage devices are much faster, they have ratios of request throughput to data bandwidth similar to those of disks from the early 1990s. Some values of the ratio, γ, of request service rate (IO/s) to streaming bandwidth (MB/s) for some recent disks include $\gamma = 26$ (1989) for the CDC Wren-IV [21], $\gamma = 17$ (1993) [12], and $\gamma = 5.2$ (1999) for the Quantum Atlas 10K [22]. γ for disks continue to drop over time as bandwidth improves faster than mechanical positioning times. In comparison, the MEMS-based storage device in this paper yields $\gamma = 19$ (1422 IO/s $\div$ 76 MB/s), comparable to disks within the last decade. Also, although many probe tips access the media in parallel, they are all limited to accessing the same relative x,y offset within a region at any given point in time—recall that the media sled moves freely while the probe tips remain relatively fixed. Thus, the probe tip parallelism provides greater data rates but not concurrent, independent accesses. There are alternative physical device designs that would support greater access concurrency and lower positioning times, but at substantial cost in capacity [11].

The remainder of this section enumerates a number of relevant similarities and differences between MEMS-based storage devices and conventional disk drives. With each item, we also discuss consequences for device management issues and techniques.

Mechanical positioning. Both disks and MEMS-based storage devices have two main components of positioning time for each request: seek and rotation for disks, X and Y dimension seeks for MEMS-based storage devices. The major difference is that the disk components are independent (i.e., desired sectors rotate past the read/write head periodically, independent of when seeks complete), whereas the two components are explicitly done in parallel for MEMS-based storage devices. As a result, total positioning time for MEMS-base storage equals the greater of the X and Y seek times, making the lesser time irrelevant. The effect of this overlap on request scheduling is discussed in Section 4.2.

Settling time. For both disks and MEMS-based storage devices, it is necessary for read/write heads to settle over the desired track after a seek. Settling time for disks is a relatively small component of most seek times (0.5 ms of 1–15 ms seeks). However, settling time for MEMS-based storage devices is expected to be a relatively substantial component of seek time (0.2 ms of 0.2–0.8 ms seeks). Because the settling time is generally constant, this has the effect of making seek times more constant, which in turn could reduce (but not eliminate) the benefit of both request scheduling and data placement. Section 4.3 discusses this issue.

Logical-to-physical mappings. As with disks, we expect the lowest-level mapping of logical block numbers (*LBNs*) to physical locations to be straightforward and optimized for sequential access; this will be best for legacy systems that use these new devices as disk replacements. Such a sequentially optimized mapping scheme fits disk terminology and has some similar characteristics. Nonetheless, the physical differences will make data placement decisions (mapping of file or database blocks to LBNs) an interesting topic. Section 5 discusses this issue.

Seek time vs. seek distance. For disks, seek times are relatively constant functions of the seek distance, independent of the start cylinder and direction of seek. Because of the spring restoring forces, this is not true of MEMS-based storage devices. Short seeks near the edges take longer than they do near the center (as discussed in Section 5). Also, turnarounds near the edges take either less time or more, depending on the direction of sled motion. As a result, seek-reducing request scheduling algorithms [34] may not achieve their best performance if they look only at distances between LBNs as they can with disks.

Recording density. Some MEMS-based storage devices use the same basic magnetic recording technologies as disks [1]. Thus, the same types of fabrication and grown media defects can be expected. However, because of the much higher bit densities of MEMS-based storage devices, each such media defect will affect a much larger number of bits. This is one of the fault management issues discussed in Section 6.1.

Numbers of mechanical components. MEMS-based storage devices have many more distinct mechanical parts than disks. Although their very small movements make them more robust than the large disk mechanics, their sheer number makes it much more likely that some number of them will break. In fact, manufacturing yields may dictate that the devices operate with some number of broken mechanical components. Section 6.1 discusses this issue.

Concurrent read/write heads. Because it is difficult and expensive for drive manufacturers to enable parallel activity, most modern disk drives use only one read/write head at a time for data access. Even drives that do support parallel activity are limited to only 2–20 heads. On the other hand, MEMS-based storage devices (with their per-tip actuation and control components) could theoretically use all of their probe tips concurrently. Even after power and heat considerations, hundreds or thousands of concurrently active probe tips is a realistic expectation. This parallelism increases media bandwidth and offers opportunities for improved reliability. Section 6.1 discusses the latter.

Control over mechanical movements. Unlike disks, which rotate at constant velocity independent of ongoing accesses, the mechanical movements of MEMS-based storage devices can be explicitly controlled. As a result, access patterns that suffer significantly from independent rotation can be better served. The best example of this is repeated access to the same block, as often occurs for synchronous metadata updates or read-modify-write sequences. This difference is discussed in Section 6.2.

Startup activities. Like disks, MEMS-based storage devices will require some time to ready themselves for media accesses when powered up. However, because of the size of their mechanical structures and their lack of rotation, the time and power required for startup will be much less than for disks. The consequences of this fact for both availability (Section 6.3) and power management (Section 7) are discussed in this paper.

Drive-side management. As with disks, management functionality will be split between host OSes and device OSes (firmware). Over the years, increasing amounts of functionality have shifted into disk firmware, enabling a variety of portability, reliability, mobility, performance, and scalability enhancements. We expect a similar trend with MEMS-based storage devices, whose silicon implementations offer the possibility of direct integration of storage with computational logic.

Speed-matching buffers. As with disks, MEMS-based storage devices access the media as the sled moves past the probe tips at a fixed rate. Since this rate rarely matches that of the external interface, speed-matching buffers are important. Further, because sequential request streams are important aspects of many real systems, these speed-matching buffers will play an important role in prefetching and then caching of sequential LBNs. Also, as with disks, most block reuse will be captured by larger host memory caches instead of in the device cache.

Sectors per track. Disk media is organized as a series of concentric circles, with outer circles having larger circumferences than inner circles. This fact led disk manufacturers to use banded (zoned) recording in place of a constant bit-per-track scheme in order to increase storage density and bandwidth. For example, banded recording results in a 3:2 ratio between the number of sectors on the outermost (334 sectors) and innermost (229 sectors) tracks in the Quantum Atlas 10K [8]. Because MEMS-based storage devices instead organize their media in fixed-size columns, there is no length difference between tracks and banded recording is not relevant. Therefore, block layout techniques that try to exploit banded recording will not provide benefit for these devices. On the other hand, for block layouts that try to consider track boundaries and block offsets within tracks, this uniformity (which was common in disks 10 or more years ago) will simplify or enable correct implementations. The subregioned layout described in Section 5 is an example of such a layout.

device capacity	3.2 GB
number of tips	6400
maximum concurrent tips	1280
sled acceleration	803.6 m/s^2
sled access speed	28 mm/s
constant settling time	0.22 ms
spring factor	75%
per-tip data rate	0.7 Mbit/s
media bit cell size	40×40 nm
bits per tip region (M×N)	2500×2440
data encoding overhead	2 bits per byte
servo overhead per 8 bytes	10 bits (11%)
command processing overhead	0.2 ms/request
on-board cache memory	0 MB
external bus bandwidth	100 MB/s

Table 1: ***Default MEMS-based storage device parameters.*** *N=2440 in order to fit an integral number of 80-bit encoded sectors (with inter-sector servo) in each column of bits. The default model includes no on-board caching (or prefetching), but does assume speed-matching buffers between the tips and the external bus.*

3 Experimental setup

The experiments in this paper use the performance model for MEMS-based storage described in Reference [11], which includes all of the characteristics described above. Although it is not yet possible to validate the model against real devices, both the equations and the default parameters are the result of extensive discussions with groups that are designing and building MEMS-based storage devices [2, 3, 20]. We therefore believe that the model is sufficiently representative for the insights gained from experiments to be useful. Table 1 shows default parameters for the MEMS-based storage device simulator.

This performance model has been integrated into the DiskSim simulation environment [10] as a disk-like storage device accessed via a SCSI-like protocol. DiskSim provides an infrastructure for exercising the device model with various synthetic and trace-based workloads. DiskSim also includes a detailed, validated disk module that can accurately model a variety of real disks. For reference, some experiments use DiskSim's disk module configured to emulate the Quantum Atlas 10K, one of the disks for which publicly available configuration parameters have been calibrated against real-world drives [8]. The Quantum Atlas 10K has a nominal rotation speed of 10,000 RPM, average seek time of 5.0 ms, streaming bandwidth of 17.3–25.2 MB/s, and average random single-sector access time of 8.5 ms [22].

Some of the experiments use a synthetically-generated workload that we refer to as the *Random* workload. For this workload, request inter-arrival times are drawn from an exponential distribution; the mean is varied to simulate a range of workloads. All other aspects of requests are independent: 67% are reads, 33% are writes, the request size distribution is exponential with a mean of 4 KB, and request starting locations are uniformly distributed across the device's capacity.

For more realistic workloads, we use two traces of real disk activity: the *TPC-C* trace and the *Cello* trace. The TPC-C trace comes from a TPC-C testbed, consisting of Microsoft SQL Server atop Windows NT. The hardware was a 300 MHz Intel Pentium II-based system with 128 MB of memory and a 1 GB test database striped across two Quantum Viking disk drives. The trace captures one hour of disk activity for TPC-C, and its characteristics are described in more detail in Reference [23]. The Cello trace comes from a Hewlett-Packard system running the HP-UX operating system. It captures disk activity from a server at HP Labs used for program development, simulation, mail, and news. While the total trace is actually two months in length, we report data for a single, day-long snapshot. This trace and its characteristics are described in detail in Reference [25]. When replaying the traces, each traced disk is replaced by a distinct simulated MEMS-based storage device.

As is often the case in trace-based studies, our simulated devices are newer and significantly faster than the disks used in the traced systems. To explore a range of workload intensities, we replicate an approach used in previous disk scheduling work [34]: we scale the traced inter-arrival times to produce a range of average inter-arrival times. When the scale factor is one, the request inter-arrival times match those of the trace. When the scale factor is two, the traced inter-arrival times are halved, doubling the average arrival rate.

4 Request scheduling

An important mechanism for improving disk efficiency is deliberate scheduling of pending requests. Request scheduling improves efficiency because positioning delays are dependent on the relative positions of the read/write head and the destination sector. The same is true of MEMS-based storage devices, whose seek times are dependent on the distance to be traveled. This section explores the impact of different scheduling algorithms on the performance of MEMS-based storage devices.

4.1 Disk scheduling algorithms

Many disk scheduling algorithms have been devised and studied over the years. Our comparisons focus on four. First, the simple *FCFS* (first-come, first-served) algorithm often results in suboptimal performance, but we include it for reference. The *SSTF* (shortest seek time first) algorithm was designed to select the request that will incur the smallest seek delay [4], but this is rarely the way it functions in practice. Instead, since few host OSes have the information needed to compute actual seek distances or predict seek times, most SSTF implementations use the difference between the last accessed LBN and the desired LBN as an approximation of seek time. This simplification works well for disk drives [34], and we label this algorithm as *SSTF_LBN*. The *CLOOK_LBN* (cyclical look) algorithm services requests in ascending LBN order, starting over with the lowest LBN when all requests are "behind" the most recent request [28]. The *SPTF* (shortest positioning time first) policy selects the request that will incur the smallest positioning delay [14, 29]. For disks, this algorithm differs from others in that it explicitly considers both seek time and rotational latency.

For reference, Figure 5 compares these four disk scheduling algorithms for the Atlas 10K disk drive and the Random workload (Section 3) with a range of request arrival rates. Two common metrics for evaluating disk scheduling algorithms are shown. First, the average response time (queue time plus service time) shows the effect on average performance. As expected, FCFS saturates well before the other algorithms as the workload increases. SSTF_LBN outperforms CLOOK_LBN, and SPTF outperforms all other schemes. Second, the squared coefficient of variation (σ^2/μ^2) is a metric of "fairness" (or starvation resistance) [30, 34]; lower values indicate better starvation resistance. As expected, CLOOK_LBN avoids the starvation effects that characterize the SSTF_LBN and SPTF algorithms. Although not shown here, age-weighted versions of these greedy algorithms can reduce request starvation without unduly reducing average case performance [14, 29].

4.2 MEMS-based storage scheduling

Existing disk scheduling algorithms can be adapted to MEMS-based storage devices once these devices are mapped onto a disk-like interface. Most algorithms, including SSTF_LBN and CLOOK_LBN, only use knowledge of LBNs and assume that differences between LBNs are reasonable approxima-

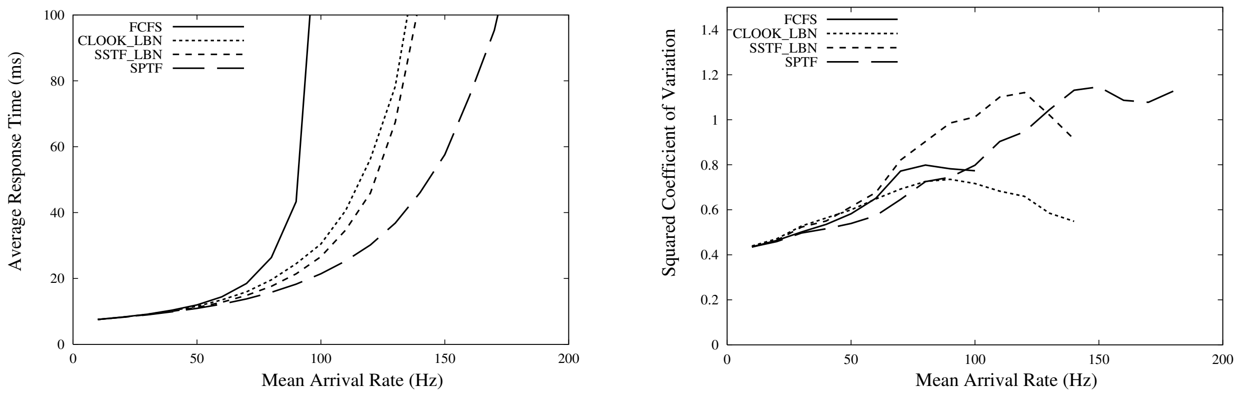

(a) Average response times

(b) Squared coefficients of variation (σ^2/μ^2)

Figure 5: ***Comparison of scheduling algorithms for the Random workload on the Quantum Atlas 10K disk.***

tions of positioning times. SPTF, which addresses disk seeks and rotations, is a more interesting case. While MEMS-based storage devices do not have a rotational latency component, they do have two positioning time components: the X dimension seek and the Y dimension seek. As with disks, only one of these two components (seek time for disks; the X dimension seek for MEMS-based storage devices) is approximated well by a linear LBN space. Unlike disks, the two positioning components proceed in parallel, with the greater subsuming the lesser. The settling time delay makes most X dimension seek times larger than most Y dimension seek times. Although it should never be worse, SPTF will only be better than SSTF (which minimizes X movements, but ignores Y) when the Y component is frequently the larger.

Figure 6 shows how well these algorithms work for the default MEMS-based storage device on the Random workload with a range of request arrival rates. In terms of both performance and starvation resistance, the algorithms finish in the same order as for disks: SPTF provides the best performance and CLOOK_LBN provides the best starvation resistance. However, their performance relative to each other merits discussion. The difference between FCFS and the LBN-based algorithms (CLOOK_LBN and SSTF_LBN) is larger for MEMS-based storage devices because the seek time is a much larger component of the total service time. In particular, there is no subsequent rotational delay. Also, the average response time difference between CLOOK_LBN and SSTF_LBN is smaller for MEMS-based storage devices, because both algorithms reduce the X seek times into the range where X and Y seek times are comparable. Since neither addresses Y seeks, the greediness of SSTF_LBN is less effective. SPTF obtains additional performance by addressing Y seeks.

Figures 7(a) and 7(b) show how the scheduling algorithms perform for the Cello and TPC-C workloads, respectively. The relative performance of the algorithms on the Cello trace is similar to the Random workload. The overall average response time for Cello is dominated by the busiest one of Cello's eight disks; some of the individual disks have differently shaped curves but still exhibit the same ordering among the algorithms. One noteworthy difference between TPC-C and Cello is that SPTF outperforms the other algorithms by a much larger margin than for TPC-C at high loads. This occurs because the scaled-up version of the workload includes many concurrently-pending requests with very small LBN distances between adjacent requests. LBN-based schemes do not have enough information to choose between such requests, often causing small (but expensive) X-dimension seeks. SPTF addresses this problem and therefore performs much better.

4.3 SPTF and settling time

Originally, we had expected SPTF to outperform the other algorithms by a greater margin for MEMS-based storage devices. Our investigations suggest that the value of SPTF scheduling is highly dependent upon the settling time component of X dimension seeks. With large settling times, X dimension seek times dominate Y dimension seek times, making SSTF_LBN match SPTF. With small settling times, Y dimension seek times are a more significant component. To illustrate this, Figure 8 compares the scheduling algorithms with the constant settling time set to zero and 0.44 ms (double the de-

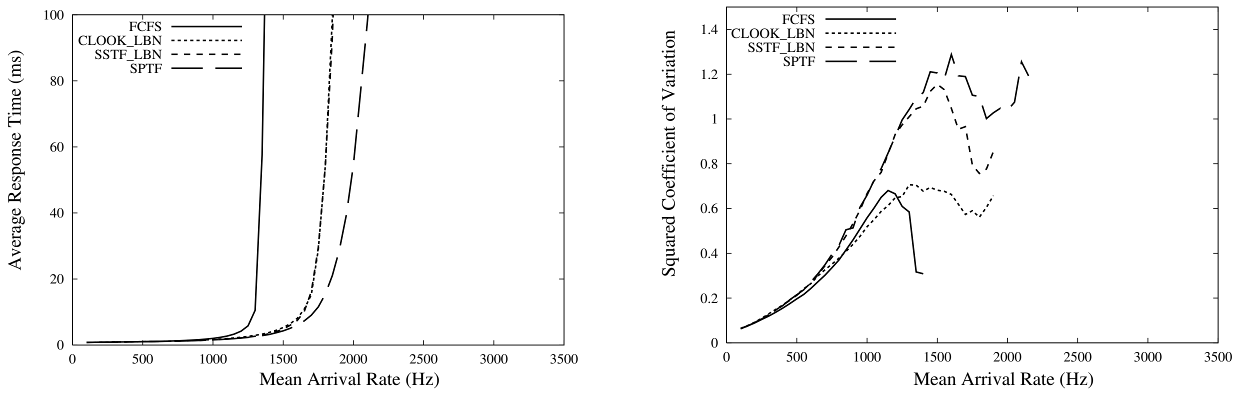

(a) Average response times

(b) Squared coefficients of variation (σ^2/μ^2)

Figure 6: ***Comparison of scheduling algorithms for the Random workload on the MEMS-based storage device.*** *Note the scale of the X axis has increased by an order of magnitude relative to the graphs in Figure 5.*

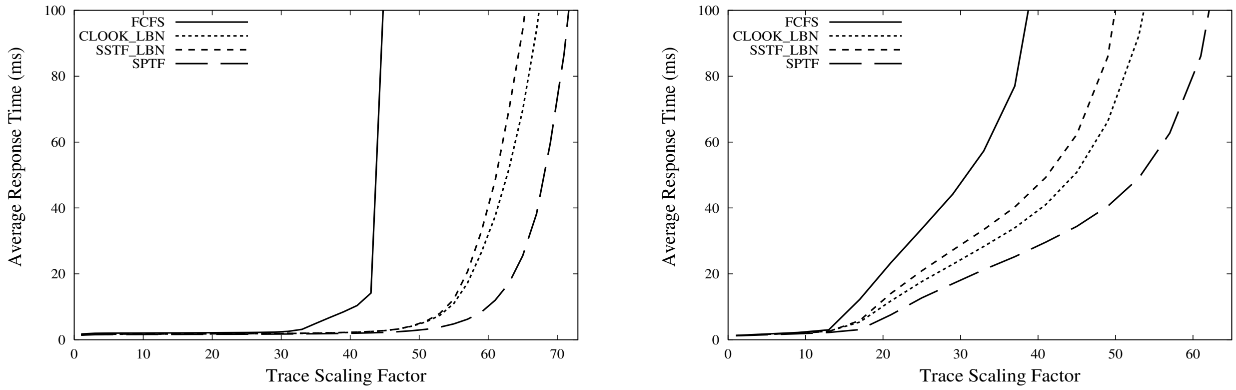

(a) Cello average response times

(b) TPC-C average response times

Figure 7: ***Comparison of scheduling algorithms for the Cello and TPC-C workloads on the MEMS-based storage device.***

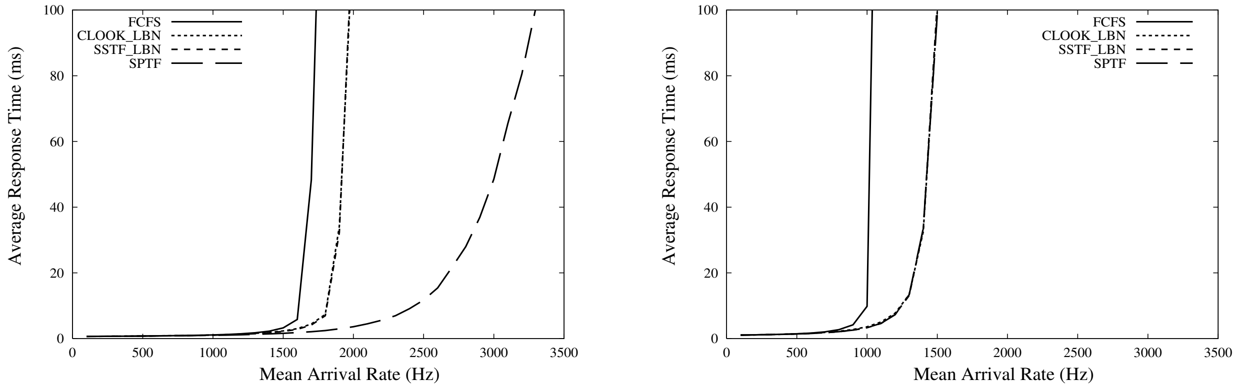

(a) Random with zero settling time

(b) Random with double settling time

Figure 8: ***Comparison of average performance of the Random workload for zero and double constant settling time on the MEMS-based storage device.*** *These are in comparison to the default model (Random with constant settling time of 0.22 ms) shown in Figure 6(a). With no settling time, SPTF significantly outperforms CLOOK_LBN and SSTF_LBN. With the doubled settling time, CLOOK_LBN, SSTF_LBN, and SPTF are nearly identical.*

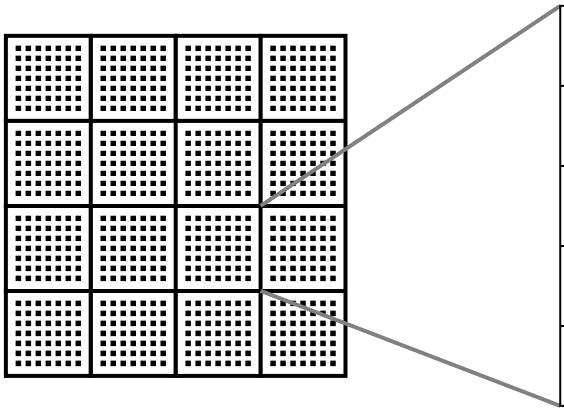

0.42	**0.39**	**0.38**	**0.39**	**0.42**
0.23	***0.21***	***0.20***	***0.21***	***0.23***
0.41	**0.38**	**0.38**	**0.38**	**0.41**
0.22	***0.20***	***0.19***	***0.20***	***0.22***
0.41	**0.38**	**0.37**	**0.38**	**0.41**
0.22	***0.20***	***0.19***	***0.20***	***0.22***
0.41	**0.38**	**0.38**	**0.38**	**0.41**
0.22	***0.20***	***0.19***	***0.20***	***0.22***
0.42	**0.39**	**0.38**	**0.39**	**0.42**
0.23	***0.21***	***0.20***	***0.21***	***0.23***

Figure 9: ***Difference in request service time for subregion accesses.*** *This figure divides the region accessible by an individual probe tip into 25 subregions, each 500×500 bits. Each box shows the average request service time (in milliseconds) for random requests starting and ending inside that subregion. The upper numbers represent the service time when the default settling time is included in calculations; numbers in italics represent the service time for zero settling time. Note that the service time differs by 14–21% between the centermost and outermost subregions.*

fault value). As expected, SSTF_LBN is very close to SPTF when the settling time is doubled. With zero settling time, SPTF outperforms the other algorithms by a large margin.

5 On-device data layout

Space allocation and data placement for disks continues to be a ripe topic of research. We expect the same to be true of MEMS-based storage devices. In this section, we discuss how the characteristics of MEMS-based storage positioning costs affect placement decisions for small local accesses and large sequential transfers. A bipartite layout is proposed and shown to have potential for improving performance.

5.1 Small, skewed accesses

As with disks, short distance seeks are faster than long distance seeks. Unlike disks, MEMS-based storage devices' spring restoring forces make the effective actuator force (and therefore sled positioning time) a function of location. Figure 9 shows the impact of spring forces for seeks inside different "subregions" of a single tip's media region. The spring forces increase with increasing sled displacement from the origin (viz., toward the outermost subregions in Figure 9), resulting in longer positioning times for short seeks. As a result, distance is not the only component to be considered when finding good placements for small, popular data items—offset relative to the center should also be considered.

5.2 Large, sequential transfers

Streaming media transfer rates for MEMS-based storage devices and disks are similar: 17.3–25.2 MB/s for the Atlas 10K [22]; 75.9 MB/s for MEMS-based storage devices. Positioning times, however, are an order of magnitude shorter for MEMS-based storage devices than for disks. This makes positioning time relatively insignificant for large transfers (e.g., hundreds of sectors). Figure 10 shows the request service times for a 256 KB read with respect to the X distance between the initial and final sled positions. Requests traveling 1250 cylinders (e.g., from the sled origin to maximum sled displacement) incur only a 10% penalty. This lessens the importance of ensuring locality for data that will be accessed in large, sequential chunks. In contrast, seek distance is a significant issue with disks, where long seeks more than double the total service time for 256 KB requests.

5.3 A data placement scheme for MEMS-based storage devices

To take advantage of the above characteristics, we propose a 25-subregion bipartite layout scheme. Small data are placed in the centermost subregions; long, sequential streaming data are placed in outer subregions. Two layouts are tested: a five-by-five grid of subregions (Figure 9) and a simple columnar division of the LBN space into 25 columns (viz., column 0 contains cylinders 0–99, column 1 contains cylinders 100–199, etc.).

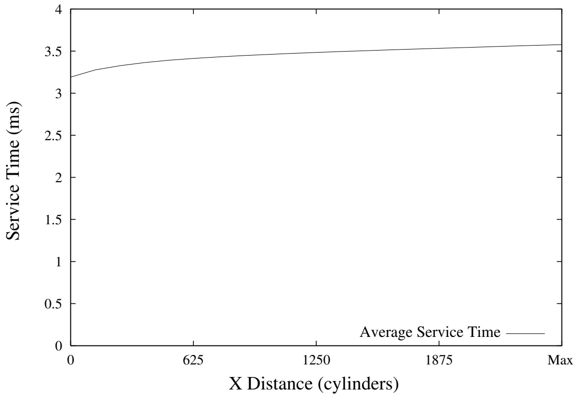

Figure 10: ***Large (256 KB) request service time vs. X seek distance for MEMS-based storage devices.*** *Because the media access time is large relative to the positioning time, seeking the maximum distance in X increases the service time for large requests by only 12%.*

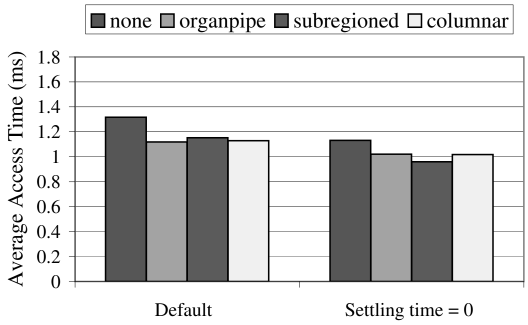

Figure 11: ***Comparison of layout schemes for MEMS-based storage devices.*** *For the default device, the organ pipe, subregioned, and columnar layouts achieve a 12–15% performance improvement over a random layout. Further, for the "settling time = 0" case, the subregioned layout outperforms the others by an additional 12%. It is interesting to note that an optimal disk layout technique does not necessarily provide the best performance for MEMS-based storage.*

We compare these layout schemes against the "organ pipe" layout [26, 32], an optimal disk-layout scheme, assuming no inter-request dependencies. In the organ pipe layout, the most frequently accessed files are placed in the centermost tracks of the disk. Files of decreasing popularity are distributed to either side of center, with the least frequently accessed files located closer to the innermost and outermost tracks. Although this scheme is optimal for disks, files must be periodically shuffled to maintain the frequency distribution. Further, the layout requires some state to be kept, indicating each file's popularity.

To evaluate these layouts, we used a workload of 10,000 whole-file read requests whose sizes are drawn from the file size distribution reported in Reference [9]. In this size distribution, 78% of files are 8 KB or smaller, 4% are larger than 64 KB, and 0.25% are larger than 1 MB. For the subregioned and columnar layouts, the large files (larger than 8 KB) were mapped to the ten leftmost and ten rightmost subregions, while the small files (8 KB or less) were mapped to the centermost subregion. To conservatively avoid second-order locality within the large or small files, we assigned a random location to each request within either the large or the small subregions. For the organ pipe layout, we used an exponential distribution to determine file popularity, which was then used to place files.

Figure 11 shows that all three layout schemes achieve a 12–15% improvement in average access time over a simple random file layout. Subregioned and columnar layouts for MEMS-based storage devices match organ pipe, even with the conservative model and no need for keeping popularity data or periodically reshuffling files on the media. For the "no settling time" case, the subregioned layout provides the best performance as it addresses both X and Y.

6 Failure management

Fault tolerance and recoverability are significant considerations for storage systems. Although MEMS-based storage devices are not yet available, MEMS components have been built and tested for many years. Their miniature size and movements will make MEMS-based storage components less fragile than their disk counterparts [17]. Still, there will likely be more defective or failed parts in MEMS-based storage because of the large number of distinct components compared to disks and the fact that bad parts cannot be replaced before or during assembly.

Although failure management for MEMS-based storage devices will be similar to failure management for conventional disks, there are several important differences. One is that individual component failures must be made less likely to render a device inoperable than in disks. Another is that MEMS-based storage devices simplify some aspects of failure management—inter-device redundancy maintenance and device restart, for example. This section discusses three aspects of failure management: internal faults, device failures, and recoverability from system crashes.

6.1 Internal faults

The common failure modes for disk drives include recoverable failures (for example, media defects or seek errors) and non-recoverable failures (head crashes, motor or arm actuator failure, drive electronics or channel failure). MEMS-based storage devices have similar failure modes with analogous causes. However, the ability to incorporate multiple tips into failure tolerance schemes allows MEMS-based storage devices to mask most component failures, including many that would render a disk inoperable.

Specifically, powerful error correcting codes can be computed over data striped across multiple tips. In our default model, each 512 byte logical block and its ECC are striped across 64 tips. This ECC can include both a horizontal component (across tips) and a vertical component (within a single sector). The horizontal ECC can recover from missing sectors. The vertical ECC identifies sectors that should be treated as missing—with the effect of converting some large errors into erasures, which can more easily be handled by the horizontal ECC. This single mechanism addresses most internal failures that are recoverable.

Media defects. In disk drives, unrecoverable media defects are handled by remapping logical block numbers to non-defective locations, with data often being lost when defects "grow" during operation. In MEMS-based storage, most media defects are expected to affect the data under a small number of tips (e.g., 1–4). Therefore, the horizontal ECC can usually be used to reconstruct unavailable bits. This capability is particularly important because the higher density of MEMS-based storage causes a given defect to affect more bits than it would in a disk. Tolerance of large media defects can be further extended by spreading each logical block's data and ECC among physically distant tips—graph coloring schemes excel at the types of data mappings required.

Tip failures. Failure of a conventional disk's read/write head or control logic generally renders the entire device inoperable. MEMS-based storage replicates these functions across thousands of components. With so many components, failure of one or more is not only possible, but probable—individual probe tips can break off or "crash" into the media, and fabrication variances will produce faulty tips or faulty tip-specific logic. Most such problems can be handled using the same mechanisms that handle media failures, since failure of a tip or its associated control logic translates into unavailability of data in the corresponding tip region. The horizontal ECC can be used to reconstruct this data.

As with disk drives, spare space needs to be withheld from the fault-free mapping of data to physical locations in MEMS-base storage. This spare space is used to store data that cannot be stored at its default physical location because of media or tip failures. The parallel operation of tips within a track provides an opportunity to avoid the performance and predictability penalties normally associated with defect remapping in disk drives. Specifically, by setting aside one or more *spare tips* in each track, unreadable sectors can be remapped to the same sector under a spare tip. A sector remapped in this way would be accessed at exactly the same time as the original (unavailable) sector would have been. In contrast, disks "slip" LBNs over defective sectors or re-map them to spare sectors elsewhere in a cylinder or zone, changing their access times relative to their original locations.

6.2 Device failures

MEMS-based storage devices are susceptible to similar non-recoverable failures as disk drives: strong external mechanical or electrostatic forces can damage the actuator comb fingers or snap off the springs, manufacturing defects can surface, or the device electronics or channel can fail. These failures should appear and be handled in the same manner as for disks. For example, appropriate mechanisms for dealing with device failures include inter-device redundancy and periodic backups.

Interestingly, MEMS-based storage's mechanical characteristics are a better match than those of disks for the common read-modify-write operations used in some fault-tolerant schemes (e.g., RAID-5). Whereas conventional disks suffer a full rotation to return to the same sector, MEMS-based storage devices can quickly reverse direction, significantly reducing the read-modify-write latency (Table 2). For the Random workload, a five-disk RAID-5 system has 77% longer response times than a four-disk striping-only system (14.3 ms vs. 8.04 ms); the latency increase for MEMS-based storage devices is only 27% (1.36 ms vs. 1.07 ms).

6.3 Recovery from host system crashes

File systems and databases must maintain internal consistency among persistent objects stored on MEMS-based storage devices, just as they do for objects on disks. Although synchronous writes will still hurt performance, the low service times of MEMS-based storage devices will lessen the penalty.

	Atlas 10K		MEMS	
# sectors	8	334	8	334
read	0.14	6.00	0.13	2.19
reposition	5.86	0.00	0.07	0.07
write	0.14	6.00	0.13	2.19
total (ms)	6.14	12.00	0.33	4.45

Table 2: ***A comparison of read-modify-write times for 4 KB (8 sector) and disk track-length (334 sector) transfers.*** *Conventional disks must wait for a complete platter rotation during read-modify-write operations, whereas MEMS-based storage devices need only perform a turnaround, a relatively inexpensive operation. This characteristic is particularly helpful for code-based redundancy schemes (for example, RAID-5) or for verify-after-write operations.*

Another relevant characteristic of MEMS-based storage devices is rapid device startup. Since no spindle spin-up time is required, startup is almost immediate—estimated at less than 0.5 ms. In contrast, high-end disk drives can take 15–25 seconds before spin-up and initialization is complete [22]. Further, MEMS-based storage devices do not exhibit the power surge inherent in spinning up disk drives, so power spike avoidance techniques (e.g., serializing the spin-up of multiple disk drives) are unnecessary—all devices can be started simultaneously. Combined, these effects could reduce system restart times from minutes to milliseconds.

7 Other considerations

This section discusses additional issues related to our exploration of OS management for MEMS-based storage devices.

Power conservation. Significant effort has gone into reducing a disk drive's power consumption, such as reducing active power dissipation and introducing numerous power-saving modes for use during idle times [6, 15, 16]. MEMS-based storage devices are much more energy efficient than disks in terms of operational power. Further, the physical characteristics of MEMS-based storage devices enable a simpler power management scheme: a single idle mode that stops the sled and powers down all non-essential electronics. With no rotating parts and little mass, the media sled's restart time is very small (estimated at under 0.5 ms). This relatively small penalty enables aggressive idle mode use, switching from active to idle as soon as the I/O queue is empty. Detailed energy breakdown and evaluation indicates that our default MEMS-based storage device employing this immediate-idle scheme would dissipate only 8–22% of the energy used by today's low-power disk drives [27].

Alternate seek control models. Our device model assumes that seeks are accomplished by a "slew plus settle" approach, which involves maximum acceleration for the first portion of the seek, followed by maximum deceleration to the destination point and speed, followed by a closed loop settling time. With such seek control, the slew time goes up as the square root of the distance and the settling time is constant (to the first order). The alternate seek control approach, a linear system seek, would incorporate rate proportional feedback to provide damping and a step input force to initiate movement to a desired location and velocity. Seeks based on such a control system exhibit longer seek times (including the settling times) that are much more dependent on seek distance [35]. This should not change our high-level conclusions, but will tend to increase the importance of both SPTF scheduling and subregion data layouts.

Erase cycles. Although our target MEMS-based storage device employs traditional rewriteable magnetic media, some designs utilize media that must be reset before it can be overwritten. For example, the IBM Millipede [31] uses a probe technology based on atomic force microscopes (AFMs), which stores data by melting minute pits in a thin polymer layer. A prominent characteristic of the Millipede design is a block erase cycle requiring several seconds to complete. Such block erase requirements would necessitate management schemes, like those used for Flash RAM devices [5], to hide erase cycle delays.

8 Summary

This paper compares and contrasts MEMS-based storage devices with disk drives and provides a foundation for focused OS management of these new devices. We describe and evaluate approaches for tuning request scheduling, data placement and failure management techniques to the physical characteristics of MEMS-based storage.

One of the general themes of our results is that OS management of MEMS-based storage devices can be similar to, and simpler than, management of disks. For example, disk scheduling algorithms can be adapted to MEMS-based storage devices in a fairly straightforward manner. Also, performance is much less dependent on such optimizations as careful data placement, which can yield order of magnitude improvements for disk-based systems [9, 19, 24]; data placement still matters, but sub-optimal solutions may not be cause for alarm. In the context of availability, internal redundancy can mask most problems, eliminating both data loss and performance loss consequences common to disk drives. Similarly, rapid restart times allow power-conservation software to rely on crude estimates of idle time.

We continue to explore the use of MEMS-based storage devices in computer systems, including their roles in the memory hierarchy [27] and in enabling new applications.

Acknowledgments

We thank Rick Carley, David Petrou, Andy Klosterman, John Wilkes, the CMU MEMS Laboratory, and the anonymous reviewers for helping us refine this paper. We thank the members and companies of the Parallel Data Consortium (including CLARiiON, EMC, HP, Hitachi, Infineon, Intel, LSI Logic, MTI, Novell, PANASAS, Procom, Quantum, Seagate, Sun, Veritas, and 3Com) for their interest, insights, and support. We also thank IBM Corporation and Intel Corporation for supporting our research efforts. John Griffin is supported in part by a National Science Foundation Graduate Fellowship.

References

[1] L. Richard Carley, James A. Bain, Gary K. Fedder, David W. Greve, David F. Guillou, Michael S. C. Lu, Tamal Mukherjee, Suresh Santhanam, Leon Abelmann, and Seungook Min. Single-chip computers with microelectromechanical systems-based magnetic memory. *Journal of Applied Physics*, **87**(9):6680–6685, 1 May 2000.

[2] Center for Highly Integrated Information Processing and Storage Systems, Carnegie Mellon University. http://-www.ece.cmu.edu/research/chips/.

[3] Data Storage Systems Center, Carnegie Mellon University. http://www.ece.cmu.edu/research/dssc/.

[4] Peter J. Denning. Effects of scheduling on file memory operations. *AFIPS Spring Joint Computer Conference* (Atlantic City, New Jersey, 18–20 April 1967), pages 9–21, April 1967.

[5] Fred Douglis, Ramon Caceres, Frans Kaashoek, Kai Li, Brian Marsh, and Joshua A. Tauber. Storage alternatives for mobile computers. *Symposium on Operating Systems Design and Implementation* (Monterey, CA), pages 25–39. USENIX Association, 14–17 November 1994.

[6] Fred Douglis, P. Krishnan, and Brian Marsh. Thwarting the power-hungry disk. *Winter USENIX Technical Conference* (San Francisco, CA), pages 292–306. USENIX Association, Berkeley, CA, 17–21 January 1994.

[7] G. K. Fedder, S. Santhanam, M. L. Reed, S. C. Eagle, D. F. Guillou, M. S.-C. Lu, and L. R. Carley. Laminated high-aspect-ratio microstructures in a conventional CMOS process. *IEEE Micro Electro Mechanical Systems Workshop* (San Diego, CA), pages 13–18, 11–15 February 1996.

[8] Greg Ganger and Jiri Schindler. Database of validated disk parameters for DiskSim. http://www.ece.cmu.edu/-~ganger/disksim/diskspecs.html.

[9] Gregory R. Ganger and M. Frans Kaashoek. Embedded inodes and explicit grouping: exploiting disk bandwidth for small files. *Annual USENIX Technical Conference* (Anaheim, CA), pages 1–17, January 1997.

[10] Gregory R. Ganger, Bruce L. Worthington, and Yale N. Patt. *The DiskSim Simulation Environment Version 1.0 Reference Manual*, CSE–TR–358–98. Department of Computer Science and Engineering, University of Michigan, February 1998.

[11] John Linwood Griffin, Steven W. Schlosser, Gregory R. Ganger, and David F. Nagle. Modeling and performance of MEMS-based storage devices. *ACM SIGMETRICS 2000* (Santa Clara, CA, 17–21 June 2000). Published as *Performance Evaluation Review*, **28**(1):56–65, June 2000.

[12] John L. Hennessy and David A. Patterson. *Computer Architecture: A Quantitative Approach, 2nd ed.* Morgan Kaufmann Publishers, Inc., San Francisco, CA, 1995.

[13] Hewlett-Packard Laboratories Storage Systems Program. http://www.hpl.hp.com/research/storage.html.

[14] David M. Jacobson and John Wilkes. *Disk scheduling algorithms based on rotational position.* HPL–CSP–91–7. Hewlett-Packard Laboratories, Palo Alto, CA, 24 February 1991, revised 1 March 1991.

[15] Kester Li, Roger Kumpf, Paul Horton, and Thomas E. Anderson. A quantitative analysis of disk drive power management in portable computers. *Winter USENIX Technical Conference* (San Francisco, CA), pages 279–291. USENIX Association, Berkeley, CA, 17–21 January 1994.

[16] Yung-Hsiang Lu, Tajana Šimunić, and Giovanni De Micheli. Software controlled power management. *7th International Workshop on Hardware/Software Codesign* (Rome, Italy), pages 157–161. ACM Press, 3–5 May 1999.

[17] Marc Madou. *Fundamentals of Microfabrication.* CRC Press LLC, Boca Raton, Florida, 1997.

[18] Marshall K. McKusick, William N. Joy, Samuel J. Leffler, and Robert S. Fabry. A fast file system for UNIX. *ACM Transactions on Computer Systems*, **2**(3):181–197, August 1984.

[19] L. W. McVoy and S. R. Kleiman. Extent-like performance from a UNIX file system. *Winter USENIX Technical Conference* (Dallas, TX), pages 33–43, 21–25 January 1991.

[20] Microelectromechanical Systems Laboratory, Carnegie Mellon University. http://www.ece.cmu.edu/~mems/.

[21] David A. Patterson, Peter Chen, Garth Gibson, and Randy H. Katz. Introduction to redundant arrays of inexpensive disks (RAID). *IEEE Spring COMPCON* (San Francisco, CA), pages 112–117, March 1989.

[22] Quantum Corporation. *Quantum Atlas 10K 9.1/18.2/36.4 GB Ultra 160/m SCSI Hard Disk Drive Product Manual*, Publication number 81-119313-05, August 6, 1999.

[23] Erik Riedel, Christos Faloutsos, Gregory R. Ganger, and David F. Nagle. Data mining on an OLTP system (nearly) for free. *ACM SIGMOD Conference 2000* (Dallas, TX), pages 13–21, 14–19 May 2000.

[24] Mendel Rosenblum and John K. Ousterhout. The design and implementation of a log-structured file system. *ACM Transactions on Computer Systems*, **10**(1):26–52,

February 1992.

[25] Chris Ruemmler and John Wilkes. UNIX disk access patterns. *Winter USENIX Technical Conference* (San Diego, CA), pages 405–420, 25–29 January 1993.

[26] Chris Ruemmler and John Wilkes. *Disk Shuffling.* Technical report HPL-91-156. Hewlett-Packard Company, Palo Alto, CA, October 1991.

[27] Steven W. Schlosser, John Linwood Griffin, David F. Nagle, and Gregory R. Ganger. Designing computer systems with MEMS-based storage. *Ninth International Conference on Architectural Support for Programming Languages and Operating Systems* (Boston, Massachusetts), 13–15 November 2000. To appear.

[28] P. H. Seaman, R. A. Lind, and T. L. Wilson. On teleprocessing system design, part IV: an analysis of auxiliary-storage activity. *IBM Systems Journal*, **5**(3):158–170, 1966.

[29] Margo Seltzer, Peter Chen, and John Ousterhout. Disk scheduling revisited. *Winter USENIX Technical Conference* (Washington, DC), pages 313–323, 22–26 January 1990.

[30] T. J. Teorey and T. B. Pinkerton. A comparative analysis of disk scheduling policies. *Communications of the ACM*, **15**(3):177–184, March 1972.

[31] P. Vettiger, M. Despont, U. Drechsler, U. Dürig, W. Häberle, M. I. Lutwyche, H. E. Rothuizen, R. Stutz, R. Widmer, and G. K. Binnig. The "Millipede"—more than one thousand tips for future AFM data storage. *IBM Journal of Research and Development*, **44**(3):323–340, 2000.

[32] Paul Vongsathorn and Scott D. Carson. A system for adaptive disk rearrangement. *Software—Practice and Experience*, **20**(3):225–242, March 1990.

[33] Kensall D. Wise. Special issue on integrated sensors, microactuators, and microsystems (MEMS). *Proceedings of the IEEE*, **86**(8):1531–1787, August 1998.

[34] Bruce L. Worthington, Gregory R. Ganger, and Yale N. Patt. *Scheduling for modern disk drives and non-random workloads.* CSE–TR–194–94. Department of Computer Science and Engineering, University of Michigan, March 1994.

[35] Pu Yang. *Modeling probe-based data storage devices.* Technical report. Department of Computer Science, University of California Santa Cruz, June 2000. Master's thesis.